HiSST: International Conference on High-Speed Vehicle Science Technology

26–29 November 2018, Moscow, Russia

Experimental and Numerical Investigation on Startup of Leading-Edge-Shaped Heat Pipes

Chen Siyuan[1], Ai Bangcheng[2], Han Haitao[3], Hu Longfei[4], Chu Min[5], Chen Liang[6]

Abstract

A kind of nickel-based superalloy/sodium heat pipe is proposed to satisfy the requirement of non-ablative thermal protection in hypersonic vehicles with sharp leading edges. As a challenge in practical application, the start-up characteristic has decisive impact on heat transfer and thermal protective performance at leading edges. Therefore, experimental researches on the heat pipe startup character are conducted. The ground tests prove the start-up property and good isothermal performance of the wedge-shaped high-temperature heat pipe. It is revealed that the charging amount of the alkali metal is one of the key factors affecting the startup characteristics of wedge-shaped heat pipes. The startup performance prediction method of wedge-shaped heat pipes is established, and the feasibility is verified by comparison with the experimental results. It is indicated that this kind of heat pipes has adaptability to the hypersonic flight environment and potential application for the thermal protection system of hypersonic vehicles.

Keywords: *high temperature heat pipe, startup, radiation heating test, numerical analysis*

Nomenclature (Tahoma 11 pt, bold)

D – flow channel characteristic size

Kn – Knudsen number

P_{sat} – saturated vapor pressure

T_{tr} – Transition temperature of the continuous vapor flow

T – cross-section temperature

κ – Boltzmann's constant

σ_0 – molecular characteristic diameter

w – circumference of the heat pipe shell

1. Introduction

High temperature heat pipes are regarded as one potential solution to non-ablative thermal protection in hypersonic vehicles with sharp leading edges. The heat pipe with high heat transfer can effectively transmit the heat from the stagnation with high heat flux to the low-heat-flow area, thus effectively reduces the stagnation temperature. Several prior development programs for hypersonic application of heat pipe have been implemented to cool the nose cap or the leading edge (Glass et al., 1999). Nearly all these concepts employed arrays of hollow circular tubes or channels. The heat pipes were bent to conform to the radius of the leading edge. so they are not compatible with sharp leading edge.

A new kind of nickel-based superalloy/sodium heat pipe with one wedge-shape chamber is proposed to satisfy the requirement of very small radius around 1 to 3mm (Li et al., 2013, Jiang et al., 2008). As illustrated in Fig.1 and Fig.2, the heat pipe composed of superalloy plates with wire mesh welded is significantly different from the traditional cylindrical heat pipe.

[1] *China Academy of Aerospace Aerodynamics(CAAA), Beijing, China 100074, siyuanbuaa@163.com,*
[2] *China Academy of Aerospace Aerodynamics(CAAA), Beijing, China 100074, stara@sohu.com*
[3] *China Academy of Aerospace Aerodynamics(CAAA), Beijing, China 100074, han_ht@139.com*
[4] *China Academy of Aerospace Aerodynamics(CAAA), Beijing, China 100074, lfhu2010@hotmail.com*
[5] *China Academy of Aerospace Aerodynamics(CAAA), Beijing, China 100074, chumin_caaa@126.com*
[6] *China Academy of Aerospace Aerodynamics(CAAA), Beijing, China 100074, clbuaa@gmail.com*

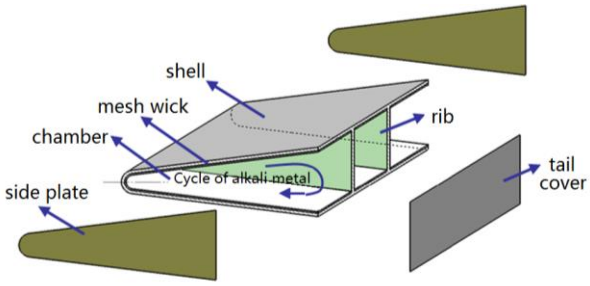

Fig 1. Schematic of wedge-shaped high-temperature heat pipe.

Fig 2. Structure of wedge-shaped high-temperature heat pipe.

As one of the main challenges in application to hypersonic vehicle, the start-up character has a decisive impact on heat transfer and thermal protective performance at leading edges (Chang, 1996, Glass et al., 1999, Glass, 1998). If the heat pipe is not activated, thermal protection structure of the leading edge will be damaged. Therefore, it is necessary to carry out the starting characteristic study. Cao and Faghri have developed a flat-front startup model for cylinder high temperature heat pipes (Cao and Faghri, 1992, Cao and Faghri, 1993, Cao and Faghri, 1992). However, the leading edge heat pipes are subjected to different degrees of aerodynamic heating on the whole outer surface, so there is no obvious evaporation section, adiabatic section, or condensing section. The analytical solution cannot be obtained according to that kind of method.

In order to verify and forecast the startup characteristic of wedge-shaped heat pipes, experimental and numerical researches on startup process are conducted. Based on the experiment results, a numerical method to analyze the startup performance is established considering the influence of the wedge shape on heat transfer and the transient non - uniform aerodynamic heating environment.

2. Experimental setup and results

2.1. Apparatus

As shown in Fig.3, the wedge-shaped heat pipe samples are locally heated by a U-shaped quartz lamp to simulate the non-uniform aerodynamic heating. The highest heat flux on the samples can reach to over 200kW/m^2. A heat flux sensor, Gordon gauge, is installed on the reflector at the back of the lamp, to acquire the change of the reference heat flux.

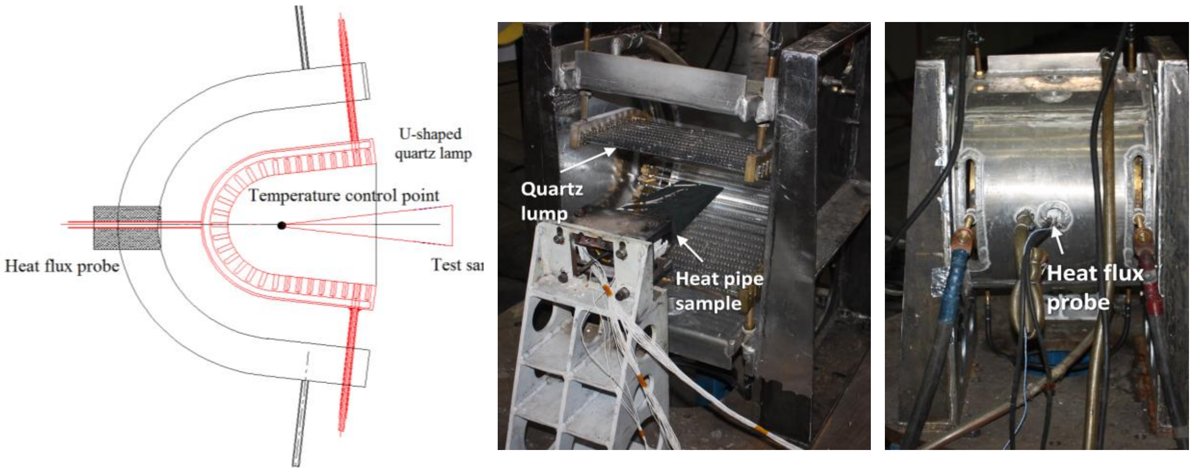

Fig 3. Experimental setup.

Three samples, which are charged with different mass of sodium, 53g,51g and 39g, separately, are tested to evaluate the effect of the filling ratio on the start-up time. These samples have the same size, 80mm x 260mm. Eight K-type thermocouples are welded on the top, side, and tail covers of the sample to measure the temperature response as shown in Fig.4. The thermocouple on the leading edge, T1, is a temperature control point used to regulate T1 temperature through the feedback control. The rise rate of T1 is set to be 7°C/s at 0~60s, 2°C /s at 60~240s, and then T1 stays at 800°C.

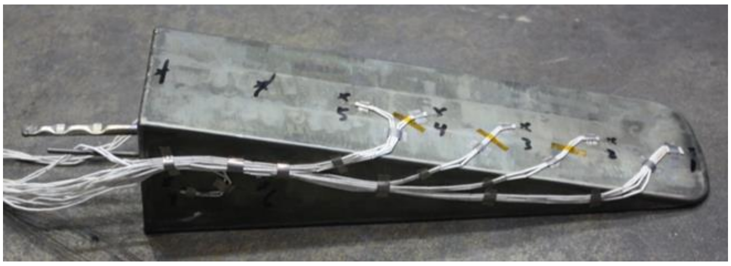

Fig 4. Test sample.

2.2. Uncertainty analysis

Uncertainty estimates are made considering the errors of the instruments, the measurement variance, and calibration errors for the heat flux and temperature measurements. The maximum variation of the 8 measured temperatures was ±0.1 C at the maximum power input. As the heat flux sensor is not implanted on the test sample, there would be deviation because of different distances. Therefore, another test was carried out to obtain the value at the same position of the sample tips. This loss varied from 15% to 3% for heat input between the minimum and maximum heat flux, respectively.

2.3. Results and discussion

The three samples with different mass of sodium are tested separately under the same temperature variation of T1 achieved by the automatic control system. The temperature response of the test points shown in 错误!未找到引用源。-10 indicates that the continue flow of the sodium vapor establishes from the head to tail in all tests, which means fully startup.

The temperature measurements and the appearance of the test sample just after radiation heating shown in Fig. 11 demonstrate the good isothermal properties of the samples under the localized heating from the quartz lamp. The heat flux measured by the probe is plotted in Fig. 12.

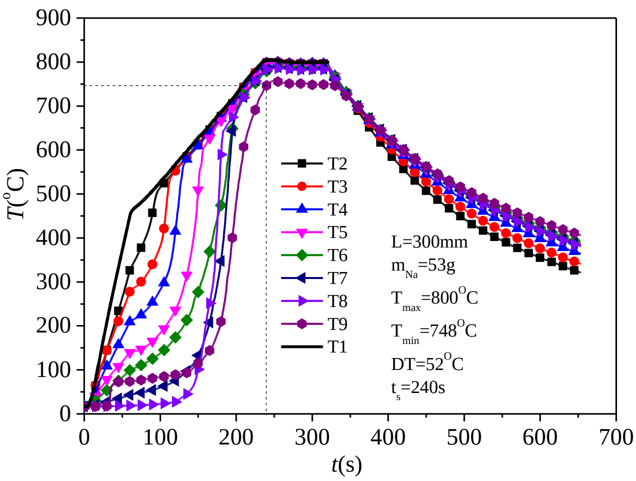

Fig 5. Temperature measurement in test 1.

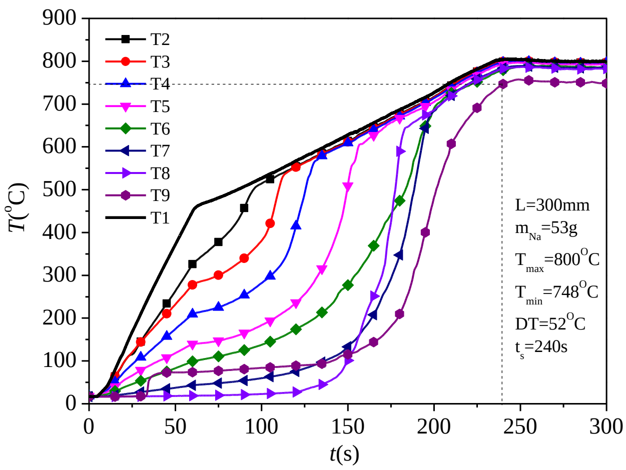

Fig 6. Startup process in test 1.

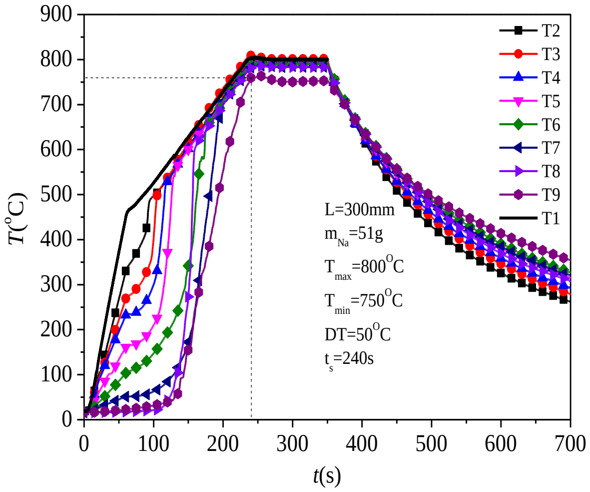

Fig 7. Temperature measurement in test 2.

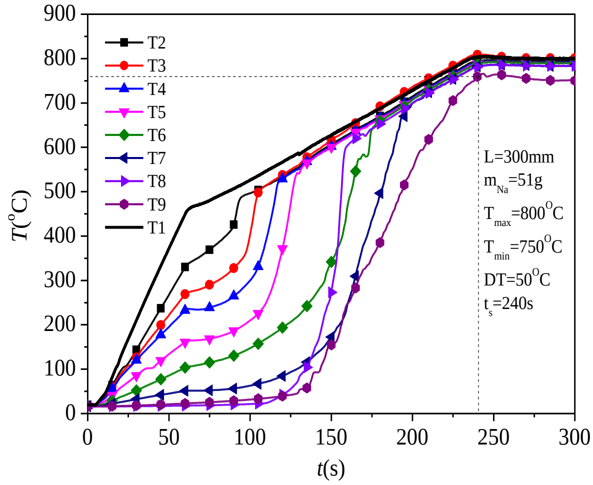

Fig 8. Startup process in test 2.

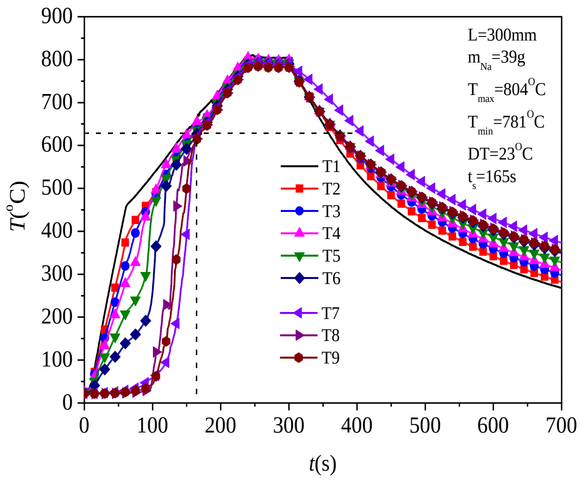

Fig 9. Temperature measurement in test 3.

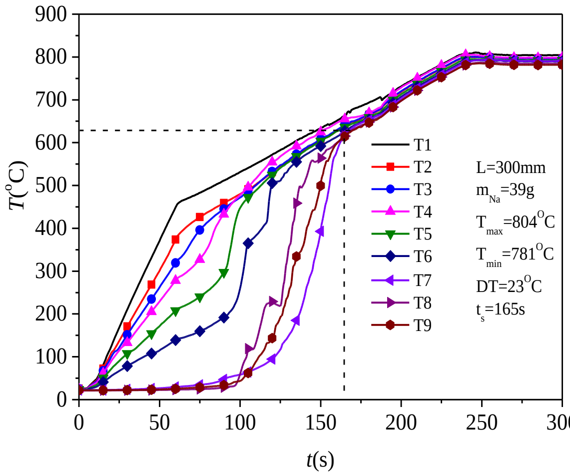

Fig 10. Startup process in test 3.

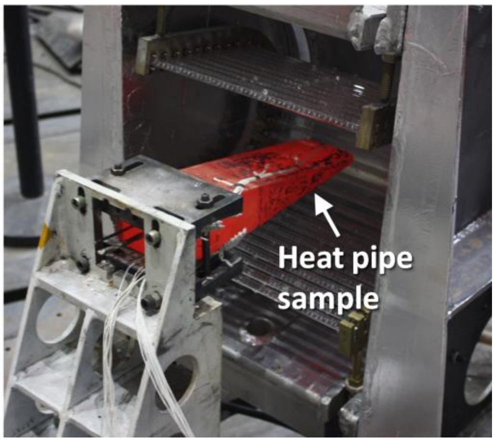

Fig 11. Post-test photograph of a test sample.

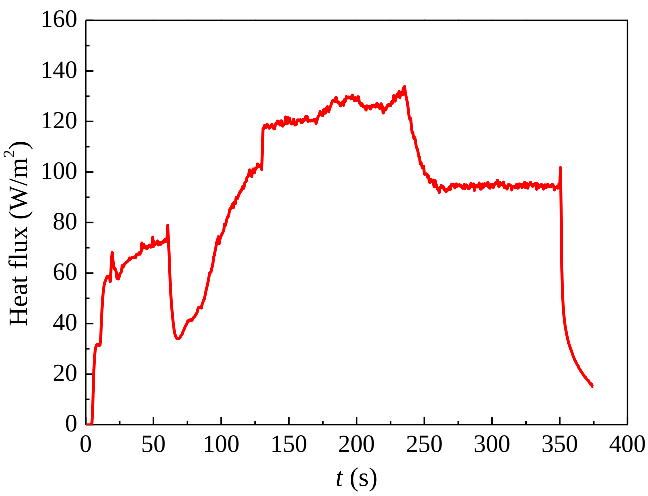

Fig 12. Heat flux measured by the probe in test 1

Table 1 indicates that the amount of charging sodium affects the startup performance of heat pipe apparently. When the charged alkali metal meets the minimum requirements, the larger the filling quantity, the longer the heat pipe start-up time and the larger the temperature difference.

Table 1. Results of three tests.

Number	Mass of sodium/g	T_{max}/°C	T_{min}/°C	△ T/°C	Time of fully Startup /s
1	53	800	748	52	240
2	51	800	750	50	240
3	39	804	781	23	165

3. NUMERICAL ANALYS

3.1. Startup model

As shown in Fig. 13, the flat-front startup model divides the high-temperature heat pipe into two regions, the high-temperature continuous flow zone and the frozen zone. The interface of the two regions is called temperature front, which is maintained at the continuous steam flow transition temperature T_{tr}. The position of the temperature front moves forward for a distance of $\triangle L$ from L_t under the heating in evaporation region. We assume that the temperature of the continuous flow zone is linear the frozen area only needs to take into account the heat conduction and the aerodynamic heating on the shell surface. Since the thickness of high temperature heat pipe shell is small, it can be assumed that the steam temperature is equal to the shell temperature at any position.

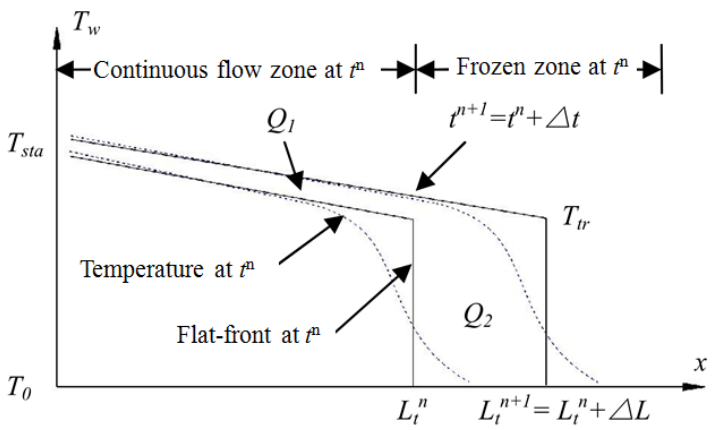

Fig 13. Schematic of the flat-front startup model for wedge-shaped heat pipe.

Different from the traditional cylinder heat pipe, all surfaces except the tail cover of leading edge heat pipes of hypersonic vehicles are under aerodynamic heating. So there is not any distinguished evaporation or condensation part in this kind of heat pipes. The aerodynamic heating, temperature rise and the steam flow state is calculated on each node, and the temperature front position and its moving distance, $\triangle L$, could be obtain based on energy conservation.

Knudsen number is usually used to represent the steam flow state in heat pipe. In this article, we assume that the steam is in a continuous flow state when $Kn \leq 0.01$. At a given temperature condition, the transition temperature T_{tr} of the continuous vapor flow and the channel characteristic size D meets the following relationship:

$$D = \frac{\kappa T}{\sqrt{2}\sigma_0^2 \mathrm{Kn} P_{sat}(T)} \tag{1}$$

For sodium heat pipes, the relationship between the continuous flow conversion temperature and the diameter of the channel section is presented in Fig. 14 using Eq. (1). For wedge-shaped heat pipes, the feature size can be approximated as the channel equivalent diameter.

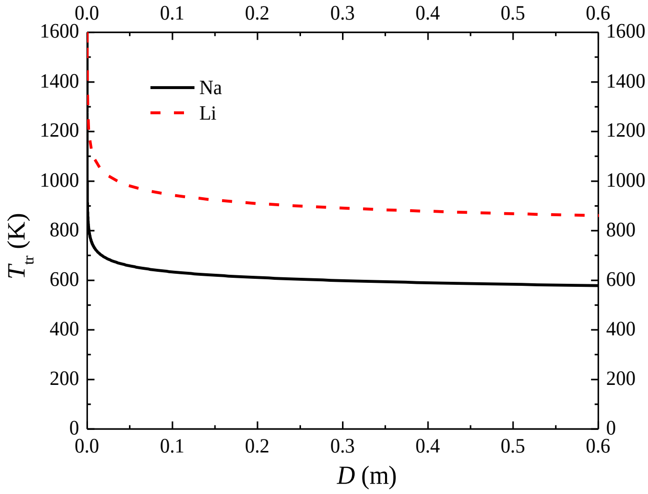

Fig 14. Transition temperatures for liquid-metal vapor flow

To satisfy energy conservation, the aerodynamic heating, Q_{input}, should be equal with the heat required, Q_{heed}, which cause the temperature rise in the continue flow region from t_n to t_{n+1}. $\triangle L$ is assumed as the moving distance from t_n to t_{n+1}, so the temperature distribution at the continue flow region and the net heat flux at t_{n+1} could be calculated. We take the average value of the aerodynamic heating at t_{n+1} and t_{n+1} as the net heat during Δt:

$$Q_{\text{input}} = \left(\int_0^{L_t^n} q_x^n dx + \int_0^{L_t^{n+1}} q_x^{n+1} dx \right) \cdot w \cdot \Delta t / 2 \tag{2}$$

Using the calculated continuous flow zone temperature distribution at two moments, the heat required in 0~ L_t^n and L_t^n~L_t^{n+1}, Q_1 and Q_2, can be obtained based on the temperature distribution at two moments. And the total heat required Q_{heed} is the sum of Q_1 and Q_2. And then, the actual value of ΔL in the current time step is adjusted by iteration to make Q_{input} equal to Q_{heed}.

3.2. Results and discussion

Comparison between the simulation results and startup test is made to validate the model. The distribution of the heat flow on the surfaces of the heat pipes is calculated according to the steady state temperature of the samples using ANSYS. The transit variations of the heating conditions are acquired from the measured heat flux by the sensor as show in Fig. 12. Therefore, the change of the heat flux distribution can be obtained.

The temperature response of the tail cover is a key indicator of the startup characteristics, reflecting the continuum flow of the alkali metal vapor. As shown in Fig. 16, the value and trend of the simulated result lies somewhere between the two thermocouples on the tail cover, T8 and T9. There are deviations of 17% and 7.7% between the simulated results and test results in the time of the jump in temperature rise rate, which represents the continuum flow arrives the tail cover. This result indicates that this kind of startup model is feasible.

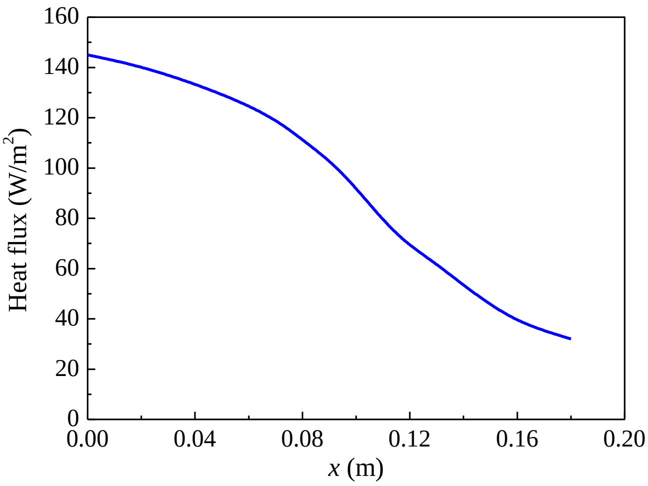

Fig 15. Heat flux distribution obtained by numerical calculation.

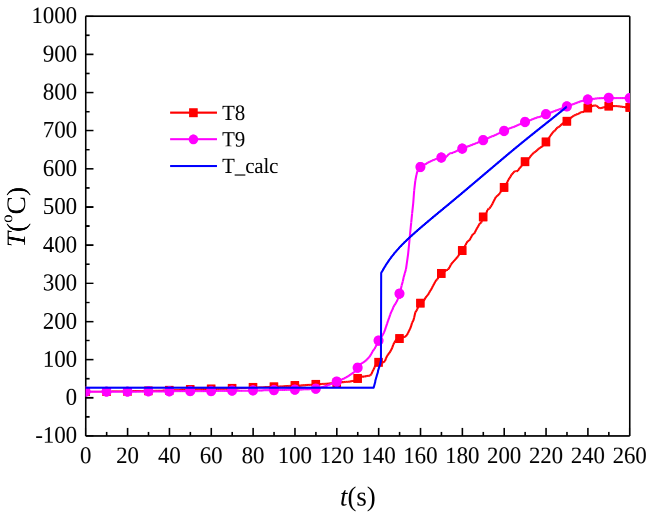

Fig 16. Comparison between simulated and test results of temperature on the cover

4. Conclusion

The ground test proves the start-up property and good isothermal performance of the wedge-shaped high-temperature heat pipe. It is proposed that this kind of heat pipes has a potential application in thermal protection system of hypersonic vehicles. Charging amount of the alkali metal is one of the key factors affecting the startup characteristics of wedge-shaped heat pipes. The startup performance prediction method of wedge-shaped heat pipes is established, and the feasibility is verified by comparison with the experimental results.

References

1. Cao, Y. and Faghri, A.: Analyses of high temperature heat pipe startup from the frozen state: Part I- numerical simulation. In 28th National Heat Transfer Conference and Exhibition, San Diego, CA, USA (1992)
2. Cao, Y. and Faghri, A.: Closed-form analytical solutions of high-temperature heat pipe startup and frozen startup limitation. Journal of heat transfer, Vol. 114, pp. 1028-1035 (1992)
3. Cao, Y. and Faghri, A.: A numerical analysis of high-temperature heat pipe startup from the frozen state. Journal of Heat Transfer, Vol. 115, pp. 247-254 (1993)

4. Chang, W. S.: Startup of the Liquid-Metal Heat Pipe in Aerodynamic Heating Environments. DTIC Document (1996)
5. Glass, D. E.: Closed Form Equations for the Preliminary Design of a Heat-Pipe-Cooled Leading Edge. NASA (1998)
6. Glass, D. E., Camarda C. J., Merrigan M. A., Sena J. T. and Reid R. S.: Fabrication and Testing of a Leading-Edge-Shaped Heat Pipe. Journal of Spacecraft and Rockets, Vol. 36, pp. 921-923 (1999)
7. Jiang, G., Ai, B. and Yu, J.: Application of high temperature heat pipe in leading thermal protections, In Proceedings of 11th China Heat Pipe Conference. Beijing (2008)
8. Li, F., Ai B. and Jiang G.: A New Thermal Protection Technology Based on Heat-Balance Isothermal Mechanism. Journal of Astronautics, Vol. 34, pp. 1644-1650 (2013)